



HAL
open science

Combining Solid State Physics Concepts and X-Ray Absorption Spectroscopy to Understand DeNOx Catalysis

Dominique Bazin, John W. Lynch, G. Treglia, Christine Mottet

► **To cite this version:**

Dominique Bazin, John W. Lynch, G. Treglia, Christine Mottet. Combining Solid State Physics Concepts and X-Ray Absorption Spectroscopy to Understand DeNOx Catalysis. *Oil & Gas Science and Technology - Revue d'IFP Energies nouvelles*, 2006, 61 (5), pp.677-689. 10.2516/ogst:2006006 . hal-00431054

HAL Id: hal-00431054

<https://hal.science/hal-00431054v1>

Submitted on 4 Feb 2019

HAL is a multi-disciplinary open access archive for the deposit and dissemination of scientific research documents, whether they are published or not. The documents may come from teaching and research institutions in France or abroad, or from public or private research centers.

L'archive ouverte pluridisciplinaire **HAL**, est destinée au dépôt et à la diffusion de documents scientifiques de niveau recherche, publiés ou non, émanant des établissements d'enseignement et de recherche français ou étrangers, des laboratoires publics ou privés.

Combining Solid State Physics Concepts and X-Ray Absorption Spectroscopy to Understand DeNO_x Catalysis

D. Bazin¹, D. Sayers^{2*}, J. Lynch³, L. Guzzi⁴, G. Trégli⁵ and C. Mottet⁵

¹ LPS, Bâtiment 510, Université Paris XI, 91405 Orsay Cedex - France.

² Department of Physics, North Carolina State University, 27695, Raleigh, North Carolina - United States

³ IFP, 1 et 4, avenue de Bois-Preau, 92852 Reuil-Malmaison Cedex - France.

⁴ Department of Surface Chemistry and Catalysis, Institute of Isotope and Surface Chemistry, CRC HAS, P.O. Box 77, 1525 Budapest - Hungary.

⁵ CRMCN, Campus de Luminy, Case 913, 13288 Marseille Cedex 9 - France.

e-mail: bazin@lps.u-psud.fr - john.lynch@ifp.fr - guzzi@sunserv.kfki.hu - treglia@crmcn.univ-mrs.fr - mottet@crmcn.univ-mrs.fr

*Many of the experimental projects of the authors were inspired by the work of Dale Sayers whose death on Nov. 25 2004 is much regretted.

Résumé — Contribution des concepts de la physique des solides et de la spectroscopie d'absorption des rayons X à la compréhension du processus de catalyse DeNO_x — Partant des considérations théoriques, l'évaluation de la variation des propriétés d'agrégats métalliques en fonction de leur taille et leur composition mène à une prédiction du mode d'adsorption du NO sur ces nanoentités. En nous appuyant sur les résultats expérimentaux obtenus surtout par la spectroscopie d'absorption de rayons X, nous proposons de lier le mode d'adsorption de la molécule au comportement de l'agrégat métallique suite à l'adsorption. Une hypothèse simple nous mène à envisager une interprétation de l'activité catalytique d'agrégats métalliques nanométriques lors de l'adsorption du NO.

Abstract — Combining Solid State Physics Concepts and X-Ray Absorption Spectroscopy to Understand DeNO_x Catalysis — Considering the NO adsorption process, starting from theoretical considerations, evaluation of the variation of the properties of metallic clusters versus their size and composition leads to a prediction of the NO adsorption mode on these nanoentities. Then, based on experimental results obtained mostly through X-ray absorption spectroscopy, we have connected the adsorption mode of the molecule to the behaviour of the metallic cluster following the adsorption process. A simple hypothesis leads us to discuss the catalytic activity of nanometer scale metallic clusters following NO adsorption.

INTRODUCTION

Nanomaterials [1] occupy a key position in the physical sciences [2, 3] in particular due to their specific surface [4, 5] and chemical [6, 7] properties. One example is supported metal catalysts [8, 9] consisting of a porous oxide such as alumina with a large specific area ($> 200 \text{ m}^2/\text{g}$) on which metal nanoparticles are dispersed. This family of materials is used in several major industrial or environmental applications [10] among which are the reduction of nitrogen oxides emitted from car exhaust systems [11, 12] and the Fischer-Tropsch synthesis [13, 14]. In order to increase the performance of these industrial processes, it is necessary to investigate the chemical reaction at the atomic level *i.e.* to understand the adsorption phenomena of small molecules on such nanoentities.

The aim of this paper is to make a bridge between solid state physics and heterogeneous catalysis, the ultimate goal being to use recent theoretical methods in solid state physics to predict the catalytic activity. The starting point is given by a brief description of the theoretical formalism developed for metallic clusters containing a small number of atoms, introducing different significant parameters such the size and the morphology as well as the possibility of relaxation of the

interatomic distances. In the following sections, we show that these structural parameters can be obtained by X-ray absorption spectroscopy (XAS) and can be affected by the preparation procedure. Then, in order to illustrate the possibilities offered by solid state physics in describing molecular adsorption processes, the adsorption of a simple molecule, NO, on nanometer-scale metallic aggregates is discussed [15-17]. More precisely, we propose that a link exists between the adsorption mode of the NO molecule and the behaviour of the metallic cluster following the NO adsorption, this behaviour being obtained from X-ray absorption studies. For transition metals which lead to dissociative adsorption, metal oxide clusters are formed. This means that the catalytic activity through the formation of nitrogen and oxygen from NO decreases significantly for these metals. On the contrary, when non dissociative adsorption is observed, a high temperature regime leads to growth of the metallic cluster. In the later case, a decrease in the catalytic activity is not observed. Thus, combining solid state physics and X-ray absorption spectroscopy seems to offer the opportunity to predict catalytic activity. Significant progress has also been achieved describing bimetallic clusters. Thus, a same approach to the prediction of catalytic activity is proposed for bimetallic systems.

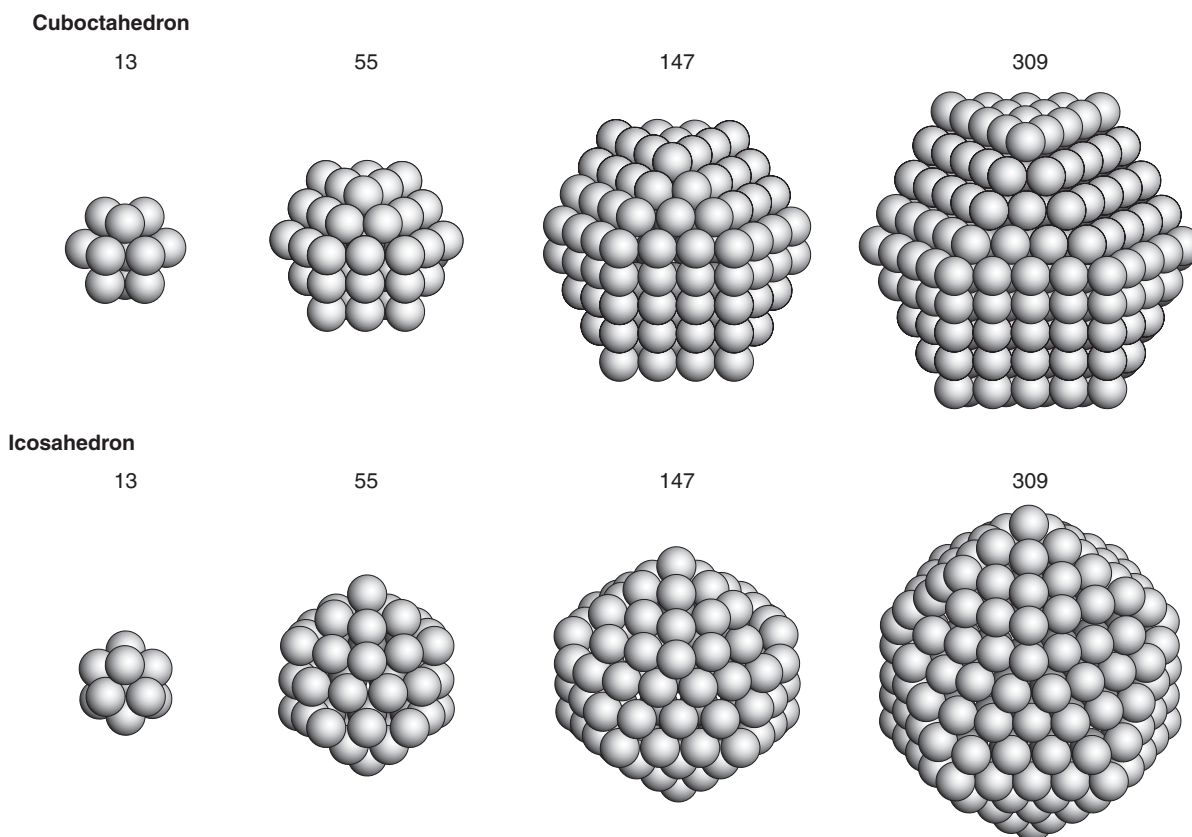


Figure 1

Cuboctahedron and icosahedron clusters containing 13, 55, 147 and 309 atoms.

1 MONOMETALLIC NANOPARTICLES

Nanometer-scale metallic clusters can first be described in terms of their geometrical properties. As underlined by several studies [18, 19], a wide range of morphologies exist. In Figure 1, clusters (icosahedron with fivefold symmetry and cuboctahedron with fcc symmetry respectively) containing a few hundred atoms are presented. In this section, we introduce some basic elements regarding the theoretical formalism associated with the calculation of the electronic structure of such entities.

1.1 Brief Description of the Theoretical Formalism

Electronic structure methods extend from *ab initio* calculations to semi-empirical models such as pseudo-potential theory for transition metals or the tight-binding approximation for transition metals. The tight-binding method starts from isolated atoms with discrete levels, which form energy bands when the atomic wave functions overlap. It assumes that any electronic state $\psi(r)$ delocalised throughout the solid, can be written as a linear combination of atomic orbitals (LCAO): $\phi_\lambda(r-n) = |n, \lambda\rangle$, where λ denotes the orbital at site n : this approximation becomes more accurate as the overlapping among the orbitals weakens (d states of transition metals).

$$\Psi(r) = \sum_{n,\lambda} a_n^\lambda \phi_\lambda(r-n) \quad (1)$$

An essential advantage of this formalism is to give a simple access to the local density of states (LDOS) at a given site n_0 from the Green function G .

$$n_{n_0}(E) = \lim_{\eta \rightarrow 0^+} \left[-\frac{\text{Im}}{\pi} \sum_{\lambda} \langle n_0, \lambda | G(E + i\eta) | n_0, \lambda \rangle \right] \quad (2)$$

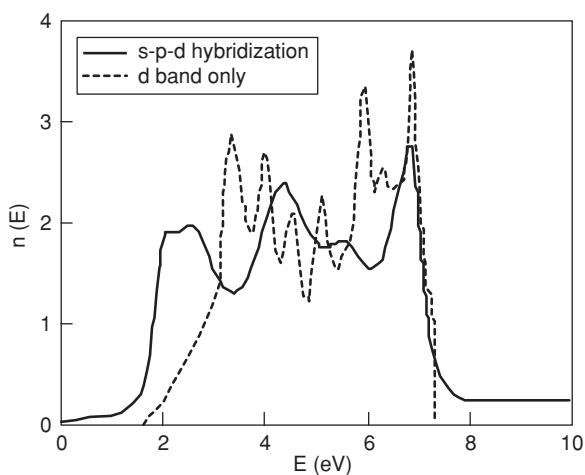


Figure 2

Pd bulk density of states, with and without sp-d hybridization, calculated in the tight-binding framework.

This concept of LDOS is particularly important for clusters since many non-equivalent sites exist at the surface (vertices, edges, facets) with various co-ordinations and atomic environments, which then define different LDOS. Note that at the end of the transition metal series, the *s* and *p* valence electrons and their hybridisation with d-orbitals have to be taken into account and that one has to be careful with charge self-consistency rules. In Figure 2 this is illustrated for Pd, for which such hybridisation is required in order to obtain a density of states in good agreement with that derived from *ab initio* calculations.

This approach also gives clear evidence that the local densities are significantly modified near the Fermi level, the amplitude of the modification depending on the site. In Figure 3, a significant size effect is observed for the Pd cluster with average density of states characteristic of a cuboctahedron (note that similar results have obtained regarding icosahedron clusters).

In parallel with the size dependence of the electronic structure, one observes inhomogeneous contractions of the cluster as well as a curvature of the facets. It is possible to obtain the equilibrium atomic configuration of the cluster at 0 K by performing a Quenched Molecular Dynamics (QMD) study in the second moment of interatomic potential. This results in the relaxation profiles shown in Figure 4 for icosahedron Pd clusters with sizes between 13 and 4000 atoms:

$$\delta R_p = \frac{R(p) - R_0(p)}{R_0(p)} \quad (3)$$

(> 0: means contraction of p shell)

where $R(p)$ is the radius of the *p*-th shell from the center ($R_0(p)$ is the value before relaxation).

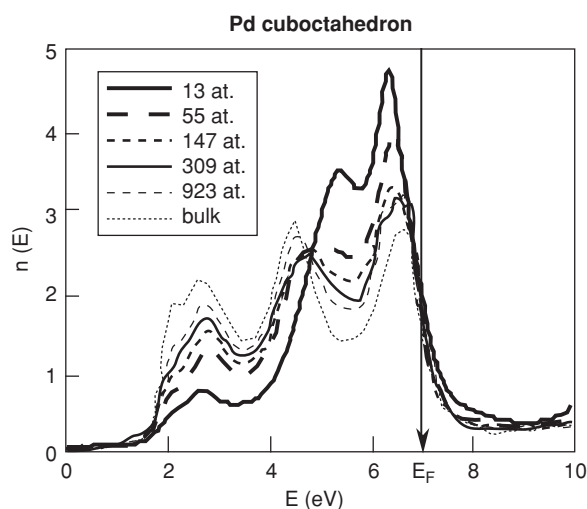


Figure 3

Size effect on the Pd cuboctahedron cluster average density of states calculated in the tight-binding formalism.

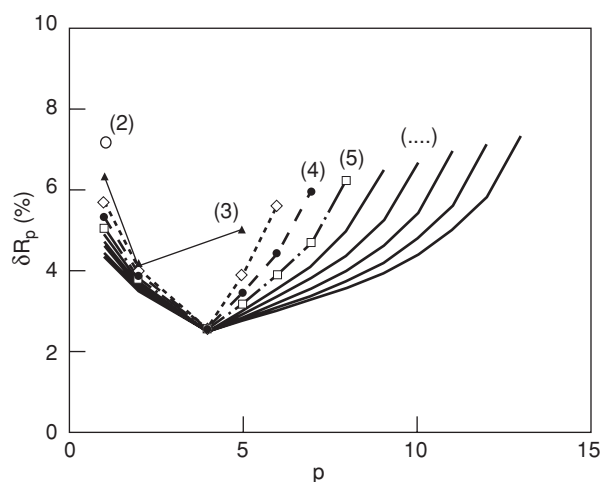


Figure 4

Radial relaxation profiles in Pd clusters, for icosahedron shapes.

Here, $\Delta R_p = \frac{R(p) - R_0(p)}{R_0(p)}$ where $R(p)$ is the radius of the p -th

shell from the centre and $R_0(p)$ is the value before relaxation.

Surprisingly, the icosahedron presents an “accordion-like” profile with a contraction both at the surface and in the core, leading to a large distribution of distances around the bulk value.

1.2 Applications to Metallic Systems

The specific properties of metal nanoparticles, such as their activity/selectivity in catalysing chemical reactions [20-22], have motivated several fundamental studies. A large number of metallic systems such as V [23], Cr [24], Fe [25], Co [26], Ni [27], Cu [28], Y [29], Rh [30], Ru [31], Pd [32] and Pt [33] have been investigated, leading to a generalised understanding of the electronic structure of different metals. Modern approaches simultaneously handle atomic and electronic structures in a consistent way by performing a relaxation process using molecular dynamics based, for example, on the method of Car and Parrinello [34].

Although in nanoparticles the electronic structure and morphology largely depend on the nature of the metal, some preferential geometries exist. For instance, in metallic Ag clusters [35], different structures coexist between 2 and 4 nm, while for Au clusters [36], only a truncated octahedron morphology has been observed. The co-existence of clusters with different geometries implies that these different species display different electronic structures (and thus different activity/selectivity properties).

Relaxation of interatomic distances with decreasing cluster size has been predicted from theoretical calculations

and confirmed by several experiments (see for example references 37 and 38). The relaxation process, however, is constrained by symmetry requirements, thus it is not homogeneous throughout the particle.

On the other hand, recent results obtained on Pd nanoparticles show a modification of the structure and morphology induced by the substrate [39, 40]. We have thus to emphasize that we are now in the position to take into account the interaction between the metallic cluster and the support (or adsorbed molecules). Lodziana and Nørskov [41] have shown that steps on the α -Al₂O₃ (0001) surface are enriched in oxygen, binding to Pd atoms and small clusters much more strongly than do the terraces. Microkinetic modeling of the NO + CO reaction on Pd particles supported on MgO [42] clearly demonstrates that the rate limiting step is, at low temperature, NO decomposition and, at high temperature, CO adsorption.

1.3 Advantages and Limitations of the X-Ray Absorption Spectroscopy

Among the different synchrotron techniques, X-ray absorption spectroscopy (XAS) [43] has several specific advantages for the study of nanomaterials.

Derived from X-ray absorption near edge spectroscopy (XANES), the electronic state of the absorbing atoms has been qualitatively linked to the density of final states to which the transitions are made. However, at least two physical phenomena affect the intensity of the “white line”: the size of the cluster, which is considered as an intrinsic effect (density of states in the platinum nanoparticles is significantly different from that of bulk Pt), and a possible charge transfer between the cluster and the support, which is considered as an extrinsic effect [44]. Thus, special attention has to be paid if a simulation of the XANES spectra is performed with a linear combination of the XANES spectra of well-crystallised reference compounds [45].

For metal nanoparticles [46] the knowledge of the different structural parameters (*i.e.* co-ordination numbers and inter-atomic distances) allows us to determine cluster size [47-49], morphology [50] and the degree of relaxation [51]. As an analysis tool, XAS [52, 53] is best suited to very small clusters [54]. The numbers of nearest neighbours vary rapidly with the diameter of the particle for such materials. For larger particles, coordination numbers are similar to those in the bulk metal. One major limitation is related to the possible existence of a distribution of sizes. It is easy to show that one set of coordination numbers may correspond to different size distributions.

Nevertheless, it should be emphasised that a unique advantage of the XAS technique is to give a precise measurement of the electronic state of the metal and to give direct structural evidence of heterometallic bonds (in the case of multimetallic systems) under *in situ* conditions, *i.e.* while the chemical reaction occurs [55, 56].

1.4 The Structural Properties of Metallic Clusters

The properties of catalysts depend on their electronic and structural characteristics, which ultimately are a function of the preparation procedure [57], the metal/support interaction, the stability of small metal nanoparticles and, last but not least, surface restructuring during the catalytic process itself.

A crucial first point is the nature of the interaction between the precursor and the support during the preparation procedure [58, 59]. For example, in manufacturing monolithic automotive catalysts, using adsorption on a washcoat of Pt nitrate, rapid adsorption occurs due to a strong interaction, leading to low dispersion, in contrast to the highly dispersed Pt obtained when H₂PtCl₆ precursor is used in reforming [60]. Note that an elegant method to point out the influence of the support on catalytic properties, based on variation of the organometallic precursor, has been proposed by Dal Santo *et al.* [61].

A large variety of metal oxides [62] have been used to stabilise and modify the electronic and structural properties of metallic clusters. Yoshitake and Iwasawa [63] have studied a range systems such as Pt/Y₂O₃, Pt/ZrO₂, Pt/V₂O₅ and Pt/TiO₂. They noticed that the modification of the density of the unoccupied 5d states of Pt strongly depends on the nature of the support.

The metal/support interaction has a strong influence on the morphology of the cluster and also on the metal-metal distance. Epitaxy between particles and the support has been observed by XAS [64]. Asakura *et al.* [65] found that platinum was stabilised in the form of raft-like nanoparticles when deposited on α -Al₂O₃(0001), as a result of direct Pt-O-Al bonding.

Recent theoretical studies have taken this interaction into account. Yamauchi *et al.* [66] evaluated the structural and electronic characteristics of Pd₃ clusters on the MgO (100) surface from quantum chemical calculations based on density functional theory (DFT). A disruption of the Pd₃ cluster may occur depending on the nature of the cluster/support interaction. More recently, Lopez *et al.* [67] performed an *ab-initio* study of metal deposition on SiO₂. The authors considered the interaction of Cu_n clusters (n = 1-5) with a non-bridging oxygen, constituting a paramagnetic point defect of silica, by DFT calculations. They predicted that the partial charge transfer to the oxide favours the formation of electrostatic interactions between the metal cluster and the oxygen atoms. Kantorovich *et al.* [68] characterised Mg clusters on MgO surfaces by *ab-initio* calculations. The calculations suggested that nucleation starts at the extended defects, *e.g.* on surface steps.

The fact that the metallic entities are generated by reduction under hydrogen alters the contraction of the interatomic distances [69] and thus the geometrical properties as well as the electronic structure of the particles. For example, Wang *et al.* [70] observed that only a small truncation occurs in the temperature range between 350°C and 450°C. Above 500°C

the particles are dramatically transformed into a spherical shape. H₂ adsorption can also modify the interaction between the cluster and the support. Deutsch *et al.* [101] pointed out that the interatomic distance between iridium and oxygen increased after treatment of the sample in H₂. Reifsnyder *et al.* [102] produced Pt clusters by heating in vacuum at 300°C and measured a contracted Pt-Pt distance (2.66 Å). When H₂ is chemisorbed, the interatomic distance is relaxed to 2.76 Å.

Finally, we have to mention the effect of the reduction temperature. Vaarkamp *et al.* [71] found by XAS that after low temperature reduction (300°C), Pt particles were 3-dimensional with a Pt-O interatomic distance of 2.7 Å. At higher temperature (450°C), the morphology of the Pt particles changed from 3-dimensional to rafts with a structure similar to the Pt (100) surface. Comparison of XAS results of Pt/zeolite samples prepared using different techniques [72] showed that the average metal particle size roughly constant (in this case 10 ± 2 Å) for reduction temperatures up to 360°C, and above this a rapid growth of metal particles is seen.

1.5 NO Adsorption on Nanometer Scale Metallic Clusters

Combining recent calculations of the electronic structure of nanometer-scale metallic clusters with the suggestion of Brown [73] relating melting point to the ability of metallic surfaces to dissociate NO, we have proposed a relationship between the adsorption mode (dissociative or molecular) of NO at room temperature and the behaviour of nanometer-scale metallic particles (sintering or disruption) in response to this adsorption. Considering a range of elements, a straight line (see Fig. 5) separates two possibilities: associative adsorption of NO accompanied by sintering of the particles and dissociative adsorption accompanied by particle fragmentation. This initial model was supported by experimental data on platinum [74-76] and ruthenium [77]. More recent data indicate that the behaviour of rhodium, iridium, palladium as well as copper is in line with this simple model.

A recent publication [78] described the interaction of NO with Rh nanoparticles supported on γ -Al₂O₃. According to X-ray absorption spectroscopy (XAS), the immediate neighbourhood of Rh atoms in the initial state is composed of 8 Rh atoms, with Rh-Rh bond length 2.68 Å. After exposure to 4% NO/He at 313 K for 5 seconds, the number of Rh-Rh bonds significantly decreased (from 8 to 2). Nitrogen atoms (N_{RhN} = 1, d_{RhN} = 1.78 Å) and oxygen atoms (N_{RhO} = 2, R_{RhO} = 2.05 Å) were present in the first coordination sphere. Comparable results were obtained previously on SiO₂-supported Rh clusters by Krause and Schmidt [79]. They showed that NO alone disperses Rh over the support. The behaviour of Rh seems to be independent of the nature of the support.

Iridium clusters have been investigated using X-ray diffraction as well as by thermal analysis. For a series of

Ir–H–ZSM-5 systems, Wögerbauer *et al.* [80] observed three different processes during interaction of NO and metallic Ir:

- decomposition of NO with formation of N₂;
- decomposition of NO with formation of N₂O;
- adsorption of NO on the Ir surface.

The dominating process depends on temperature. Moreover, through a set of experiments performed at 500°C, they showed that NO in contact with Ir⁰ was decomposed to N₂ with concurrent oxidation of Ir⁰ to IrO₂. Their work underlines the influence of another key parameter, the crystallite size.

In the case of a recent study on nanometer scale copper clusters [81], the sample was prepared by a method different from the classical impregnation technique. A 5 Å γ -Al₂O₃ film was created by exposing the clean surface of a stoichiometric NiAl{110} crystal to oxygen and heating to 1200 K, produced a sharp LEED pattern characteristic of the Al₂O₃ structure. Copper was then evaporated from a bead source made by melting high-purity Cu wire wrapped around a tungsten filament. The adsorption and reaction of NO on the Cu clusters was studied using infrared, molecular beam, and scanning tunnelling spectroscopies over the temperature range of 90–300 K. The adsorption mode of NO was studied by IR spectroscopy. At low coverage two main bands were observed, at 1586 and 1500 cm⁻¹, associated respectively with two distinct monomeric NO species, adsorbed in two-fold bridge sites on (110) type facets and three-fold hollow sites on facets which resemble (111) surfaces.

An interesting case is given by a metal of the second transition group *i.e.* palladium. On a perfect Pd(111) surface, NO adsorbs molecularly [82] while molecular adsorption and dissociation strongly compete on Pd(100) [83] and Pd(110) [84] surfaces. Finally, the stepped Pd(311) surface is active for the thermal dissociation of NO [85]. Thus it seems that the position of this metal close to the straight line in our interpretation is coherent with the high structural sensitivity of the ability of a Pd surface to dissociate NO. For nanometer scale Pd particles, no overall morphological changes of the nanocrystals were observed during NO gas exposure [86]. Thus it seems that the straight line can be considered as a “structural stability” line.

As a preliminary conclusion, while this simple model was first supported by a set of experimental data on Pt and Ru, it seems that the behaviour of Rh, Ir, Cu and Pd clusters following the NO adsorption process is also in line with this simple scheme.

We would like now to address the effect of temperature on NO adsorption and propose physicochemical mechanisms. The starting point of this discussion is the work of Asakura *et al.* [65] who used XAS to study the structural transformation of Pt clusters on α -Al₂O₃ (0001) on NO adsorption. A nondissociative adsorption of NO on Pt clusters is observed. Moreover, the initial Pt raft is destroyed to form monomer species by the interaction with NO.

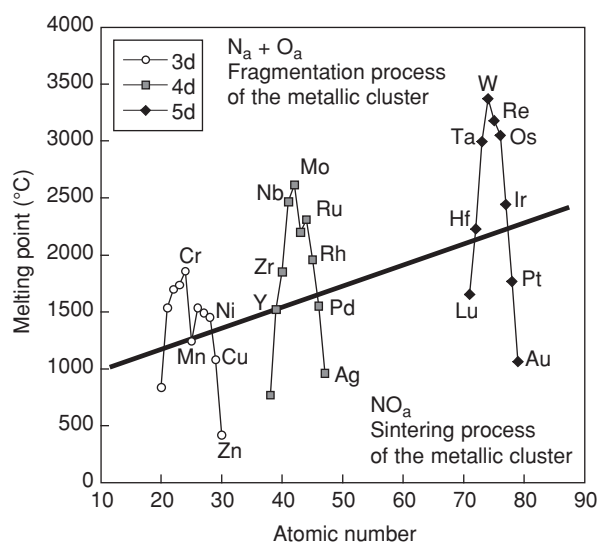


Figure 5

Diagram showing a suggested correlation [15] between the adsorption mode and the behaviour of metallic clusters. The thick straight line represents the frontier between dissociative adsorption with fragmentation (above the line) and associative adsorption with sintering (below the line).

Here we wish to propose, even if there is so far no unambiguous structural evidence of this hypothesis, two different mechanisms which can explain the link between the adsorption mode of the molecule and the structural behaviour of the nanocluster.

When we consider metals below the straight line in Figure 5, after the initial state given by nanometer scale metallic cluster in presence of molecular NO, a non-dissociative adsorption mode occurs. If the temperature is low, then we may observe a structural situation close to the one observed by Asakura *et al.* [65] in the case of platinum *i.e.* monomer species linked to several NO molecules. Then, with increase of temperature, the mobility of the nitrosyl species over the surface of the support leads to the formation of large clusters.

When we consider metals above the “stability” line, a dissociative adsorption mode occurs. According to the work of Campbell *et al.* [78] the metallic atoms may have bonds either to oxygen or nitrogen atoms. At high temperature, the formation of a metallic oxide can be observed due to desorption of nitrogen species (as N₂ molecules).

We would like now to discuss the validity of the “stability” line which separates the two regimes for the NO adsorption. When a diatomic molecule such as NO approaches a metal surface [3], it may encounter three kinds of potential wells corresponding respectively to a physisorbed state (far from the surface), a molecular chemisorbed state and

finally to a dissociative chemisorption state. Molecular chemisorption is the most stable situation if:

$$|E_{\text{ads}}(\text{N})| + |E_{\text{ads}}(\text{O})| < E_{\text{dis}}(\text{NO}) + |E_{\text{ads}}(\text{NO})| \quad (4)$$

where $E_{\text{ads}}(X)$ is the atomic adsorption energy (< 0) of atom X while $E_{\text{dis}}(\text{NO})$ and $E_{\text{ads}}(\text{NO})$ are respectively the dissociation energy (> 0) of the free molecule and the molecular chemisorption energy (< 0). The dissociation energy $E_{\text{diss}}(\text{NO})$ is clearly independent of the nature of the metal. As adsorption energies increase, the two atomic adsorption terms on the left hand side of Equation 4 eventually come to dominate the single molecular adsorption term on the left hand side and dissociative chemisorption becomes more stable. Thus the variation of adsorption mode along a transition series may be rationalised on the basis that the adsorption energies are higher for metals which are at the middle of the transition series, metals for which we observed here a dissociative adsorption.

1.6 Relation Between the Purely Energetic Model and Catalytic Activity

Is it possible to extract some information regarding the activity of the metallic clusters from this purely energetic approach? For a first family of metals (above the stability line), the final structural characteristic of the supported phases is a metal oxide. Assuming that the metal oxide has no catalytic activity, the rate of conversion of NO molecules would tend to be quite low. Such a conclusion is in line with the experimental results obtained by Campbell *et al.* [78].

On the contrary, in the case of the second family of metals (below the line) large metallic clusters are finally generated. Let's suppose that the metallic part of the cluster consists of a mixture of very small and large clusters. We may suppose that the first participate in the growth process after the adsorption of NO and thus do not contribute to catalytic activity. With time, the small particles disappear to form large ones. Following this hypothesis, the behaviour of the activity versus time may pass through a maximum as underlined by the work of Garcia-Cortès *et al.* [87].

2 BIMETALLIC CLUSTERS

As pointed out by Barbier *et al.* [88], from an experimental point of view, the preparation procedure of bimetallic catalysts influences the type of interaction between the two metallic species. For example, electrochemical methods can be used to bring the two metals into close contact [89].

Modelling of catalytic reactions for a bimetallic cluster requires knowledge both of morphology, as is the case for monometallic entities, and of local chemical ordering before interaction with adsorbed molecules can be addressed [90].

It is firstly important to predict the equilibrium structure of the particles, since breaking the bulk symmetry leads to both atomic and chemical rearrangements. Unfortunately, it is not easy to treat both on the same level.

2.1 Effect of Finite Size on Surface Segregation

Qualitatively, one expects that two effects play an important role. Firstly, we have to consider the effect of a finite number of atoms of each type. This is important for dilute systems when the available quantity of the element tending to segregate may be lower than the number of available surface sites. In this case, even if all atoms of one component are segregated to the surface, full coverage is not achieved. This may be the case for small particle size leading to a high surface/bulk ratio. Secondly, there is a geometrical effect due to the coexistence of facets with different orientations. This results in mixed concentration profiles which could be antagonistic, leading to anti-phases boundaries.

2.2 Pt-4d-Metal Clusters

For Pt-4d metal binary systems, it is necessary to develop another type of approximation, which will only be suited to study the effect of chemical ordering on a rigid lattice. Compared to monometallic systems, the total energy of the alloy, for a given configuration, cannot be described by a sum of pair interactions. Nevertheless, a (small) part of the energy which depends explicitly on configuration (essential due to ordering) can be described in an Ising-like form by developing the energy with perturbation with respect to that of the disordered state: as treated within the Coherent Potential Approximation (CPA) [91]. For bimetallic systems A-B possessing non-equivalent sites, such as extended surfaces or clusters, one obtains:

$$E_{\text{coh}}(\{p_n^i\}) = \bar{E}(c) + \sum_{n,i} p_n^i h_n^i + \frac{1}{2} \sum_{n,m,i,j} p_n^i p_m^j V_{nm}^{ij} \quad (5)$$

in which a linear term and a quadratic one appear with respects to occupation numbers P_n^i which are equal to 1 if site n is occupied by an atom of type i , and to zero if not. Both terms are calculated from the electronic structure of the disorder state described in the CPA approximation. Due to broken bonds, the equilibrium concentration on the various non-equivalent sites has no reason to be the same as in the bulk either for a surface (phenomenon of surface segregation) or for vertex, edge, facet and core sites in clusters. In that case, the segregation energy, *i.e.* the energy balance involved when exchanging a core atom with one at a p -site ($p = \text{vertices, edges, facets}$), only requires the knowledge of two parameters. The first one, issued from the linear term, is the variation of the site energy between the two pure

elements (surface energy in the case of surface segregation: $\tau^A - \tau^B$). The second one, linked to the quadratic term, is nothing but the linear combination:

$$V_{nm} = \frac{1}{2}(V_{nm}^{AA} + V_{nm}^{BB} - 2V_{nm}^{AB})$$

which can be used to calculate the mixing or ordering energies of the system under study, but not its cohesive energy. Moreover, V_{nm} decreases rapidly with the distance ($n-m$) so that its sign for first neighbour interactions ($V_{nm} = V$) indicates the tendency to order ($V > 0$) or phase-separate ($V < 0$).

It is easy to extend the Tight Binding Ising Method (TBIM) to this finite state by replacing layer concentrations by shell concentrations in which the shell i has N_i sites. One can divide the surface shell into four sub-shells corresponding to vertices ($p = 1$), edges ($p = 2$), (100) and (111) facets ($p = 3, 4$). To simplify, let us first assume that the concentrations are homogeneous and depend only on coordination: $c_p = c_c$ (the concentration in the “core”) for $p > 4$ (sites other than surface sites). The concentration profile is then given by:

$$\frac{c_p}{1-c_p} = \frac{c_c}{1-c_c} \exp\left(-\frac{\Delta E_p(c_1, \dots, c_c)}{kT}\right) \quad (6)$$

The effect of finite matter appears on the matter conservation rule, since now there is no longer an infinite reservoir. If dispersion is defined by:

$$D_p = \frac{N_p}{N_{tot}}$$

this rule allows c_c and then c_p to be determined.

$$c_c \left(1 - \sum_{p=1}^4 D_p\right) = c_c - \sum_{p=1}^4 \frac{c D_p}{c_c + (1-c_c) \exp\left(\frac{\Delta E_p(c_1, \dots, c_c)}{kT}\right)} \quad (7)$$

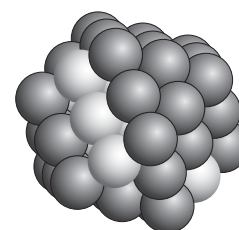
Moreover, there may exist a competition between ordering and surface tension effects. This is illustrated in Figure 6 showing the results of Monte Carlo simulations in the TBIM potential for Pt-Pd clusters [92] at sufficiently low temperature ($T = 10$ K). It is known that this system presents a tendency to ordering and that Pd should segregate due to its lower surface tension ($\tau^{Pd} < \tau^{Pt}$). For small clusters consisting of 55 atoms and two concentrations (PtPd₂ cuboctahedron, Pt₃Pd icosahedron) Pd is first segregated to the sites with low coordination (vertices, edges, etc.). For larger clusters of 923 atoms of concentration Pt₆Pd₄, Pd occupies successively the vertices, the edges, then square facets, but it begins to occupy bulk sites before the triangular sites are filled, which allows the L10 ordered structure to be preserved. As a result, one finds many non-equivalent surface sites, leading to some local order specific to the size and concentration.

In a recent paper [93], we limited ourselves to the treatment of Pt-M bimetallic systems where M is a 4d transition metal. The chosen sequence allows us to consider

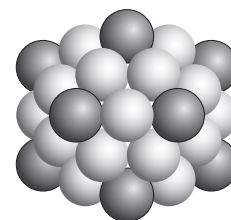
systems which present respectively a strong tendency to chemical ordering (M = Mo: $V \gg 0$), a weaker one (M = Pd, Rh: $V > 0$) and a tendency to phase separation (M = Ru, $V < 0$).

Recently published studies show that progress in theoretical physics now allows the distribution of metals inside bimetallic nanoparticles to be predicted, at least in the case of compounds of elements chosen at the end of transition metal series. Although we are concerned with a description at thermodynamic equilibrium, the predicted distribution of the metals between the core and the surface of the particles is in general consistent with experimental data, despite the system being affected by preparation parameters such as the nature of the precursor.

As a conclusion, this model can be used as a useful starting point for the preparation of such objects, even though, up to now, very few studies dedicated to bimetallic clusters have undertaken on this type of theoretical basis.



Cuboctahedron PtPd₂ (55 atoms)



Icosahedron Pt₃Pd (55 atoms)

Figure 6

Competition between segregation and ordering in PtPd clusters (Pt atoms are white, Pd atoms are black): cuboctahedron (left) and icosahedron (right).

2.3 Other Bimetallic Systems

Bimetallic clusters are increasingly the subject of experimental measurement [94-96]. Renouprez *et al.* [97] described the catalytic activity of a series of silica-supported Pd-Ni catalysts in the hydrogenation of 1,3-butadiene, for which pure palladium is an order of magnitude more active than pure nickel. The surface composition was measured by low

energy ion scattering (LEIS). The results were in agreement with the theoretical predictions for bulk alloys based on thermodynamic calculations, once these are corrected for the effect of particle size, and show the migration of palladium from the bulk to the surface of the particles. Zhu *et al.* [98] reported a study on the structure of bimetallic Pd_{0.5}Cu_{0.5} clusters, using X-ray diffraction and computer simulations. The structures obtained in the simulations exhibit face-dependent surface segregation, and alternating layers rich in one of the metals. As an example regarding electronic structure, in the bimetallic system Pt-Sn/SiO₂, quantum chemical calculations employing density functional theory (DFT) for Pt₁₉ and Pt₁₆Sn₃ clusters confirmed experimental evidence that Sn donates electrons to the 6s, 6p and 5d orbitals of platinum [99, 100]. It is important to underline that information regarding the electronic transfer between a molecule and the metal is also potentially available.

2.4 Advantages and Limitations of XAS Regarding Bimetallic Systems

Several studies have been performed on bimetallic systems using XAS because this is one of the few techniques capable of revealing the distribution of the two metals inside a nanometer scale cluster. In the case of a homogeneous system for which the core of the cluster is composed of N_A atoms of type A and the surface consists of N_B atoms of type B, the total coordination ($N_{AA} + N_{AB}$ for A atoms, $N_{BA} + N_{BB}$ for B atoms) is equal to 12 for A atoms, and less than 12 for B atoms [45]. More specifically, in the case of bimetallic clusters, the following relationships apply:

$$N_{AA} + N_{AB} = 12 > N_{BA} + N_{BB}, N_A * N_{AB} = N_B * N_{BA} \quad (8)$$

Nevertheless, this property is no longer valid when monometallic clusters coexist with bimetallic ones. We have previously pointed out that the number of heterobonds decreases significantly as the content of monometallic cluster increases. If most of the atoms A are involved in monometallic clusters, we have $N_{AA} + N_{AB} < N_{BA} + N_{BB}$ and thus the supposed distribution of the two metals inside the cluster, derived from the different coordination values as if only bimetallic cluster existed, is simply false. This point has never been clearly addressed in various experimental studies on bimetallic clusters.

2.5 The Catalytic Activity of Bimetallic Clusters

XAS experiments performed at the Pt L_{III} edge have been carried out recently on two catalysts: a monometallic 1 wt% Pt and a bimetallic 1 wt% Pt-1 wt% Rh system. Under an atmosphere of 1% NO in N₂, strong sintering of Pt particles was observed above 473 K, while for Pt-Rh particles this sin-

tering process was not observed [14]. At the start of the process, the presence of Pt-Rh bonds is clearly shown by the shape of the Fourier transform modulus (Fig. 7). Oxidation of the bimetallic particles then takes place. It is thus clear that the presence of Rh in the environment of Pt significantly modifies the behaviour of the particles during the NO adsorption process.

The question now arises whether it is possible to explain the behaviour of the bimetallic cluster using Figure 5. A possible approach is to consider a straight line between platinum and rhodium on the diagram proposed for monometallic systems. In the Pt rich region, the behaviour of PtRh bimetallic clusters will be similar to the Pt monometallic system whereas, in the Rh rich region, their behaviour will be similar to the Rh monometallic system. If we consider now the experimental result obtained on the 1% Pt-1% Rh bimetallic system, we see that this result is in line with the conclusion obtained with this simple approach.

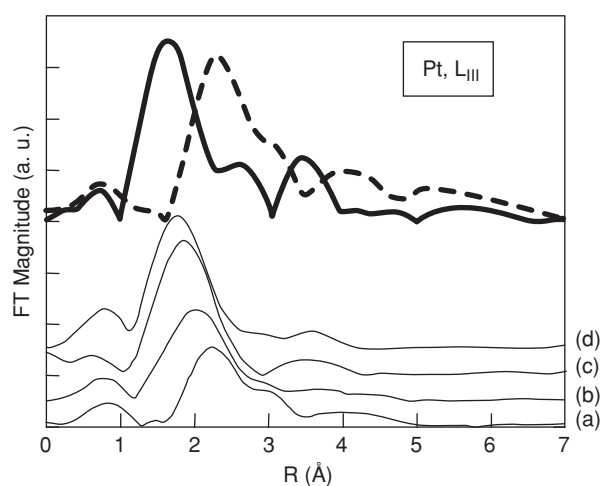


Figure 7

FT magnitude of the reduced PtRh catalyst at 25°C (a), under NO+N₂ at 100°C (b), 200°C (c) and 300°C (d). Thick solid line: PtO₂ reference, thick dashed line: Pt metal reference.

CONCLUSION

Recent theoretical calculations provide important information on the electronic structure and morphology of metal nanoparticles. The key goals are to understand the morphology of the cluster, the distribution of the two metals inside bimetallic clusters and the electronic transfer between two metals as well as between adsorbed molecules and atoms at the cluster surface. It is thus quite clear that the experimental data obtained by X-ray absorption spectroscopy can help in an

understanding at the atomic level. Analysis conditions enable the preparation to be followed and mimicking different chemical processes will give opportunities to optimise several industrial processes.

Regarding the NO adsorption process, starting from surface science considerations, the theoretical evaluation of the variation of the cohesion energy of metallic clusters versus their size allows us a knowledge of the NO adsorption mode on these nanoentities. Then, based on experimental results obtained mostly through X-ray absorption spectroscopy, we have connected the adsorption mode of the molecule to the behaviour of the metallic cluster following the adsorption process. This simple hypothesis leads us to discuss the catalytic activity of nanometer scale metallic cluster regarding the NO adsorption process. Research work to confirm or modify this simple model is in progress.

ACKNOWLEDGEMENTS

The authors are indebted to Dr. D. Spanjaard from the Laboratoire de Physique des Solides (*Paris XI University*, France), Dr. M.C. Desjonqueres (from the *CEA-Saclay*), Dr. F. Garin, Dr. G. Maire from the *LERCSI* (Strasbourg, France), Dr. C. Pichon, Dr. B. Rebours, Dr. R. Revel for the *IFP*, Dr. A. Seigneurin, Dr. Y. Klur, Dr. A. Pourpoint from *Rhodia* (Aubervilliers, France), Dr. M. Capelle, Dr. F. Maire, Dr. G. Meunier, Dr. R. Noirot, from *PSA Peugeot-Citroën* (Centre technique de Belchamp, France) for invaluable discussions on the topic of nanometer-scale clusters.

Also, the authors are indebted to the Hungarian Science and Research Fund (T-034920) for financial support and the COST D15/0005/99 program and the Chemistry Department of the *CNRS* for supporting a collaborative program with *LURE* synchrotron facilities.

REFERENCES

- Somorjai, G.A. (2004) On the Move, *Nature*, **430**, 730.
- Friedel, J. (1978) *Physics of Metals*, Cambridge University Press, Cambridge.
- Desjonqueres, M.C. and Spanjaard, D. (1998) *Concepts in Surface Physics*, Springer-Verlag, Berlin.
- Sinfelt, J. (2002) Role of surface science in catalysis. *Surf. Sci.*, **500**, 923.
- Zaera, F. (2001) Probing catalytic reactions at surfaces, *Prog. Surf. Sci.*, **69**, 1.
- Thomas, J.M. and Thomas, W.J., (1997) *Principles and Practice of Heterogeneous Catalysis*, Wiley-VCH Verlag GmbH & Co. KGaA, Weinheim.
- Iwasawa, Y. (2003) *In situ* characterization of supported metal catalysts and model surfaces by time-resolved and three-dimensional XAFS techniques, *J. Catal.*, **216**, 165.
- Somorjai, G.A. and McCrea, K. (2001) Roadmap for catalysis science in the 21st century: a personal view of building the future on past and present accomplishments. *Appl. Catal. A-Gen.*, **222**, 3.
- Gates, B.C. (2000) Supported nanostructured catalysts: Metal complexes and metal clusters. *J. Mol. Catal. A-Chem.*, **163**, 55.
- Russell, A.E. and Rose, A. (2004) X-ray absorption spectroscopy of low temperature fuel cell catalysts, *Chem. Rev.*, **104**, 4613.
- Pârvulescu, V.I., Grange, P. and Delmon, B. (1998) Catalytic removal of NO. *Catal. Today*, **46**, 233.
- Garin, F. (2001) Environmental catalysis, *Appl. Catal. A-Gen.*, **222**, 183.
- Dry, M.E. (1981) The Fischer-Tropsch Synthesis in *Catalysis Sciences and Technology*, Anderson, J.R. and Boudart, M., (Eds.) **1**, Springer Verlag, Berlin, 159.
- Van Wechem, V.M.H. and Senden, M.M.G., (1994) Conversion of natural gas to transportation fuels via the Shell Middle Distillate Process, *Stud. Surf. Sci. Catal.*, **81**, 43.
- Bazin, D., Mottet, C., Tréglia, G. and Lynch, J. (2000) New trends in heterogeneous catalysis processes on metallic clusters from synchrotron radiation and theoretical studies, *Appl. Surf. Sci.* **164**, 140.
- Bazin, D. (2002) Solid state concepts to understand catalysis using nanoscale metallic particles, *Top. Catal.*, **18**, 79.
- Bazin, D. (2003) Solid State Physics and Synchrotron Radiation Techniques to Understand Heterogeneous Catalysis in nanotechnology, Ed. G.A. Somorjai, S. Hermans, B. Zhou, Ed. kluwer.
- Ino, A. (1969) Stability of multiply-twinned particles *J. Phys. Soc. Jpn*, **27**, 941.
- Wulff, G.V. (1901) Zur frage der Geschwindigkeit des Wachstums und der Auflösung der Krystallflächen, *Z. Krystallogr.*, **34**, 449.
- Pesant, L., Matta, J., Garin, F., Ledoux, M.J., Bernhardt, P., Pham, C. and Pham-Huu C. (2004) A high-performance Pt/SiC catalyst for catalytic combustion of model carbon particles (CPs). *Appl. Catal. A-Gen.*, **266**, 21.
- Nohair, B., Especel, C., Marécot, P., Montassier, C., Hoang, L.C., and Barbier, J. (2004) Selective hydrogenation of sunflower oil over supported precious metals. *C. R. Acad. Sci. II C*, **7**, 113.
- Henry, C. (2000) Catalytic activity of supported nanometer-sized metal clusters, *Appl. Surf. Sci.*, **164**, 252.
- Alvarado, P., Dorantes-Davila, J.L. and Pastor G.M. (1998) Magnetic properties of 3d transition-metal nanostructures: Cr and V clusters embedded in bulk Fe, *Phys. Rev. B*, **58**, 12116.
- Reddy, B.V., Khanna, S.N. and Jena, P. (1999) Structure and magnetic ordering in Cr₈ and Cr₁₃ clusters, *Phys. Rev. B* **60**, 15598.
- Oda, T., Pasquarello, A. and Car, R. (1998) Fully unconstrained approach to noncollinear magnetism: Application to small Fe clusters, *Phys. Rev. Lett.*, **80**, 3622.
- Guirado-Lopez, R. (2001) Magnetic anisotropy of fcc transition-metal clusters: Role of surface relaxation, *Phys. Rev. B*, **63**, 174420.
- Calleja, M., Rey, C., Alemany, M.M.G., Gallego, L.J. Ordejon, P., Sanchez-Portal, D., Artacho, E. and Soler, J.M. (1999) Self-consistent density-functional calculations of the geometries, electronic structures, and magnetic moments of Ni-Al clusters, *Phys. Rev. B*, **60**, 2020.
- Mottet, C. Tréglia, G. and Legrand, B. (1997) New magic numbers in metallic clusters: an unexpected metal dependence, *Surf. Sci. Lett.*, **383**, L719.

- 29 Guirado-Lopez, R., Desjonqueres, M.C. and Spanjaard, D. (1999) Electronic and magnetic structure in 4d transition metal clusters, *Appl. Surf. Sci.*, **144**, 663.
- 30 Barreateau, C., Spanjaard, D. and Desjonqueres, M.C. (1999) Electronic structure and energetics of transition metal surfaces and clusters from a new spd tight-binding method, *Surf. Sci.*, **433**, 751.
- 31 Guirado-Lopez, R., Desjonqueres, M.C., Spanjaard, D. and Aguilera-Granja, F. (1998) Electronic and geometrical effects on the magnetism of small Ru_N clusters, *J. Magn. Magn. Mat.*, **186**, 214.
- 32 Mottet, C., Tréglia, G. and Legrand, B. (1996) Electronic structure of Pd cluster in the tight-binding approximation: influence of spd hybridization, *Surf. Sci.*, **352**, 675.
- 33 Khoutami, A. (1993) PhD, University of Paris XI.
- 34 Car, R. and Parrinello, M. (1985) Unified Approach for Molecular Dynamics and Density-Functional Theory, *Phys. Rev. Lett.*, **55**, 2471.
- 35 Hall, B.D., Flueli, M., Monot, R. and Borel, J.P. (1991) Multiply twinned structures in unsupported ultrafine silver particles observed by electron diffraction, *Phys. Rev. B*, **43**, 3906.
- 36 Pinto, A., Pennisi, A.R., Faraci, G., D'agostino, G., Mobilio, S. and Boscherini, F. (1995) Evidence for truncated octahedral structures in supported gold clusters, *Phys. Rev. B*, **51**, 5315.
- 37 Apai, G., Hamilton, J.F., Stohr, J. and Thompson, A. (1979) Exafs of small Cu and Ni clusters: Binding-energy and bond-length changes with cluster size, *Phys. Rev. Lett.*, **13**, 165.
- 38 Moraweck, B., Clugnet, G. and Renouprez, A.J. (1979) Contraction and relaxation of interatomic distances in small platinum particles from extended X-ray absorption fine structure (EXAFS) spectroscopy, *Surf. Sci.*, **81**, L631.
- 39 Vervish, W., Mottet, C. and Goniakowski, J. (2002) Theoretical study of the atomic structure of Pd nanoclusters deposited on a MgO(100) surface, *Phys. Rev. B*, **65**, 245411.
- 40 Mottet, C., Goniakowski, J., Baletto, F., Ferrando, R. and Tréglia, G. (2004) Modeling free and supported metallic nanoclusters: Structure and dynamics, *Phase Transit.*, **77**, 101.
- 41 Lodziana, Z. and Nørskov, J.K. (2002) Interaction of Pd with steps on Al₂O₃ (0001), *Surf. Sci.*, **518**, L577.
- 42 Prevot, G. and Henry, C.R. (2002) Microkinetic modeling of the CO + NO reaction on Pd/MgO particle, *J. Phys. Chem. B*, **106**, 12191.
- 43 Sayers, D.A., Lytle, F.W. and Stern, E.A. (1970) *Advances in X-ray Analysis*, Ed. Plenum, New-York, 13, 1970.
- 44 Bazin, D., Sayers, D., Rehr, J., Mottet, C. (1997) Numerical simulation of the Pt L_{III} edge white line relative to nanometer scale clusters. *J. Phys. Chem.*, **100**, 5332.
- 45 Bazin, D., Rehr, J.J. (2003) Limits and advantages of X-ray absorption near edge structure for nanometer scale metallic clusters, *J. Phys. Chem. B* **107**, 12398.
- 46 Bazin, D., Lynch, J., Ramos-Fernandez, M. (2003) Xas and Amax: Two basic tools in heterogeneous catalysis, *Oil Gas Sci. Technol.*, **58**, 683.
- 47 Clausen, B.S., Grabaek, L., Topsoe, H., Hansen, L.B., Stoltze, P., Nørskov, J.K. and Nielsen, O.H. (1993) A new procedure for particle size determination by EXAFS based on molecular dynamics simulations, *J. Catal.*, **141**, 368.
- 48 Ramallo-López, J.M., Requejo, F.G., Craievich, A.F., Wei, J., Avalos-Borja, M. and Iglesia, E. (2005) Complementary methods for cluster size distribution measurements: supported platinum nanoclusters in methane reforming catalysts, *J. Mol. Catal. A-Chem.*, **228**, 299.
- 49 Womes, M., Cholley, T., Le Peltier, F., Morin, S., Didillon, B., and Szydłowski-Schildknecht, N. (2005) Study of the reaction mechanisms between Pt(acac)₂ and alumina surface sites: Application to a new refilling technique for the controlled variation of the particle size of Pt/Al₂O₃ catalysts, *Appl. Catal. A-Gen.*, In Press.
- 50 Jacobs, G., Ghadiali, F., Pisanu, A., Borgna, A., Alvarez, W.E. and Resasco, D.E (1999) Characterization of the morphology of Pt clusters incorporated in a KL zeolite by vapor phase and incipient wetness impregnation. Influence of Pt particle morphology on aromatization activity and deactivation, *Appl. Catal. A-Gen.*, **188**, 79.
- 51 Frenkel, A.I., Hills, C.W., and Nuzzo, R.G. (2001) A view from the inside: Complexity in the Atomic Scale Ordering of Supported Metal Nanoparticles, *J. Phys. Chem. B.*, **105**, 12689.
- 52 Chao, K.J., and We, A.C. (2001) Characterization of heterogeneous catalysts by X-ray absorption spectroscopy, *J. Electron Spectroscopy and Related Phenomena*, **119**, 175.
- 53 Stakheev, A.Y. and Kustov, L.M. (1999) Effects of the support on the morphology and electronic properties of supported metal clusters: modern concepts and progress in 1990s, *Appl. Catal. A-Gen.*, **188**, 3.
- 54 Bazin, D., Sayers, D., Rehr, J. (1997) Comparison between Xas, Amax, Asaxs & Dafs applied to nanometer scale metallic clusters, *J. Phys. Chem.*, **101**, 11040.
- 55 Lynch, J. (2002), Development of structural characterisation tools for catalysts. *Oil Gas Sci. Technol.*, **57**, 281.
- 56 Grunwaldt, J.D., Caravati, M., Hannemann, S. and Baiker, A. (2004) X-ray absorption spectroscopy under reaction conditions: suitability of different reaction cells for combined catalyst characterization and time-resolved studies, *Phys. Chem. Chem. Phys.*, **6**, 3037
- 57 Shih, C.C. and Chang, J.R. (2005) Genesis and growth of platinum subnano-particles on activated-carbon characterized by X-ray absorption spectroscopy: effects of preparation conditions, *Mater. Chem. Phys.*, **92**, 89-97.
- 58 Yao, N., Pinckney, C., Lim, S., Pak, C. and Haller, G.L. (2001) Synthesis and characterization of Pt/MCM-41 catalysts, *Micropor. Mesopor. Mat.*, **44-45**, 377.
- 59 Chen, Y., Ciuparu, D., Lim, S., Yang, Y., Haller, G.L. and Pfefferla, L. (2004) Synthesis of uniform diameter single-wall carbon nanotubes in Co-MCM-41: effects of the catalyst pre-reduction and nanotube growth temperatures, *J. Catal.*, **225**, 453.
- 60 Dou, D., Liu, D.J., Williamson, W.B., Kharas, K.C. and Robota, H.J. (2001) Structure and chemical properties of Pt nitrate and application in three-way automotive emission catalysts, *Appl. Catal. B-Environ.*, **30**, 11.
- 61 Dal Santo, V., Dossi, C., Recchia, S., Colavita, P.E., Vlaic, G. and Psaro, R. (2002) Carbon tetrachloride hydrodechlorination with organometallics-based Pt and Pd catalysts on MgO, *J. Mol. Catal. A-Chem.*, **182-183**, 157.
- 62 Benfield, R.E., Grandjean, D., Dore, J.C., Esfahanian, H., Wu, Z., Kröll, M., Geerkens, M. and Schmid, G. (2004) Structure of assemblies of metal nanowires in mesoporous alumina membranes studied by EXAFS, XANES, X-ray diffraction and SAXS, *Faraday Discuss.*, **125**, 327.
- 63 Yoshitake, H. and Iwasawa, Y. (1992) Electronic metal support interaction in platinum catalysts under deuterium-ethene reaction conditions and the microscopic nature of the active sites, *J. Phys. Chem. B*, **96**, 1329.

- 64 Bazin, D., Dexpert, H., Guyot-Sionnest, N.S., Bournonville, J.P. and Lynch, J. (1989) Exafs characterization of reforming catalysts: examples of recent applications, *J. Chim. Phys.*, **7**, 86.
- 65 Asakura, K., Chun, W.J., Shirarai, M., Tomishige, K. and Iwasawa, Y. (1997) In-situ polarization-dependent total-reflection fluorescence XAFS studies on the structure Transformation of Pt Clusters on $\text{Al}_2\text{O}_3(0001)$, *J. Phys. Chem. B*, **101**, 5549.
- 66 Yamauchi, R., Gunji, I., Endou, A., Yin, X., Kubo, M., Chatterjee, A. and Miyamoto, A. (1998) Electronic and structural features of Pd₃ cluster on MgO(100) surface cluster, *Appl. Surf. Sci.*, **130**, 572.
- 67 Lopez, N., Illas, F. and Pacchioni, G. (1999) Electronic effects in the activation of supported metal clusters: Density functional theory. study of H₂ dissociation on Cu/SiO₂, *J. Phys. Chem. B*, **103**, 1712.
- 68 Kantorovich, L., Shluger, A., Günster, J., Stultz, J., Krischok, S., Goodman, D.W., Stracke, P., and Kemper, V. (1999) Mg clusters on MgO surfaces: characterization by MIES and electronic structure ab initio calculations, *Nucl. Instrum. Meth. B*, **157**, 162.
- 69 Montano, P.A., Schulze, W., Tesche, B., Shenoy, G.K. and Morrison T.I. (1984) Exafs study of Ag particles isolated in solid argon, *Phys. Rev.*, **30**, 672.
- 70 Wang, Z.L., Petroski, J.L., Green, T.C. and El-Sayed, M.A. (1998) Shape transformation and surface melting of cubic and tetrahedral Platinum nanocrystals, *J. Phys. Chem. B*, **32**, 6145.
- 71 Vaarkamp, M., Miller, J.T., Modica, F.S. and Koningsberger, D.C. (1996) On the relation between particle morphology, structure of the metal-support Interface, and catalytic properties of Pt/ Al_2O_3 , *J. Catal.* **163**, 294.
- 72 Pandya, K.I., Heald, S.M., Hriljac, J.A., Petrakis, L. and Fraissard, J. (1996) Characterization by EXAFS, NMR, and other techniques of Pt/NaY Zeolite at industrially relevant low concentration of Platinum, *J. Phys. Chem. B*, **100**, 5070.
- 73 Brown, W. and King, D.A. (2000) NO chemisorption and reactions on metal surfaces: a new perspective, *J. Phys. Chem. B*, **104**, 2578.
- 74 Schneider, S., Bazin, D., Garin, F., Maire, G., Dexpert, H., Meunier, G., Noiro, R. and Capelle, M. (1999) NO reaction over nanometer scale platinum clusters deposited on γ -alumina: an XAS study, *Appl. Catal.*, **189**, 39.
- 75 Loof, P., Stenbom, B., Norden, H. and Kasemo, B. (1993) Rapid Sintering in NO of Nanometer-Sized Pt Particles on small γ - Al_2O_3 Observed by CO Temperature-Programmed Desorption and Transmission Electron Microscopy, *J. Catal.*, **44**, 60.
- 76 Wang, X., Sigmon, S.M., Spivey, J.J. and Lamb, H.H. (2004) Support and particle size effects on direct NO decomposition over platinum, *Catal. Today*, **96**, 11.
- 77 Hashimoto, T., Hayashi, H., Udagawa, Y. and Ueno, A. (1995) NO induced morphology changes by Xafs study, *Physica B*, **208/209**, 683.
- 78 Campbell, T., Dent, A.J., Diaz-Moreno, S., Evans, J., Fiddy, S.G., Newton, M.A. and Turin, S. (2002) Susceptibility of a heterogeneous catalyst, Rh/ Al_2O_3 , to rapid structural change by exposure to NO, *Chem. Commun.*, **30**, 304-305.
- 79 Krause, K.R., and Schmidt, L.D. (1993) Microstructural changes and volatilization of Rh and Rh/Ce on SiO₂ and Al_2O_3 in NO + CO, *J. Catal.*, **140**, 424.
- 80 Wögerbauer, C., Maciejewski, M. and Baiker, A. (2002) Structure Sensitivity of NO Reduction over Iridium Catalysts in HC-SCR, *J. Catal.*, **205**, 157.
- 81 Haq, S., Carew, A. and Raval, R. (2004) Nitric oxide reduction by Cu nanoclusters supported on thin Al_2O_3 films, *J. Catal.*, **221**, 204.
- 82 Ramsier, R.D., Gao, Q., Neergaard Waltenburg, H., Lee, K.W., Nooij, O.W., Lefferts, L. and Yates, J.T. (1994) NO adsorption and thermal behavior on Pd surfaces. A detailed comparative study, *Surf. Sci.*, **320**, 209.
- 83 Sugai, S., Watanabe, H., Kioka, T., Miki, H. and Kawasaki, K. (1991) Chemisorption of NO on Pd(100), (111) and (110) surfaces studied by AES, UPS and XPS, *Surf. Sci.*, **259**, 109.
- 84 Sharpe, R.G. and Bowker, M. (1996) The adsorption and decomposition of NO on Pd(110), *Surf. Sci.*, **360**, 21.
- 85 Nakamura, I., Fujitani, T. and Hamada, H. (2002) Adsorption and decomposition of NO on Pd surfaces, *Surf. Sci.*, **514**, 409.
- 86 Højrup Hansen, K., Sljivananin, Z., Laesgsgaard, E., Besenbacher, F. and Stensgaard, I. (2002) Adsorption of O₂ and NO on Pd nanocrystals supported on $\text{Al}_2\text{O}_3/\text{NiAl}(110)$: overlayer and edge structures, *Surf. Sci.*, **505**, 25.
- 87 Garcia-Cortès, J.M., Pérez-Ramirez, J., Rouzaud, J.N., Vaccaro, A.R., Illán-Gómez, M.J. and Salinas-Martinez de Lecea, C. (2003) On the structure sensitivity of deNOx HC-SCR over Pt-beta catalysts, *J. Catal.*, **218**, 111.
- 88 Barbier, J., Chollier, M.J. and Epron, F. (1997) In "Catalysis by Metals" Renouprez, A.J. and Jovic, H. (Eds.), EDP Sciences-Springer.
- 89 Barbier, J. (1992) Redox reactions in the tailoring of bimetallic catalysts in *Advances in Catalyst Preparation*, Catalytic Studies Division, Mountain View, California.
- 90 Derosa, P.A., Seminario, J.M. and Balbuena, P.B. (2001) Properties of Small Bimetallic Ni-Cu Clusters, *J. Phys. Chem. A*, **105**, 7917.
- 91 Trégliã, G., Legrand, B., Ducastelle, F., Saúl, A., Gallis, C., Meunier, I., Mottet, C. and Senhaji, A. (1999) Alloy surfaces: segregation, reconstruction and phase transitions, *Comp. Mater. Sci.*, **15**, 196.
- 92 Khoutami, A., Legrand, B., Mottet, C. and Trégliã, G. (1994) On the influence of topology on the energy profile in metallic Pd clusters, *Surf. Sci.*, **307-309**, 735.
- 93 Bazin, D., Mottet, C. and Trégliã, G. (2000) New opportunities to understand heterogeneous catalysis processes through synchrotron radiation studies and theoretical calculations of density of states: The case of nanometer scale bimetallic particles, *Appl. Catal. A-Gen.*, **200**, 47.
- 94 Garcia-Gutierrez, D.I., Gutierrez-Wing, C.E., Giovanetti, L.E., Ramallo-Lopez, J.M., Requejo, F.G. and Jose-Yacamán, M. (2005) Temperature Effect on the Synthesis of Au-Pt Bimetallic Nanoparticles, *J. Phys. Chem. B*, **109**, 3813.
- 95 Nutt, M.O., Hughes, J.B. and Wong, M.S. (2005) Designing Pd on Au bimetallic nanoparticles catalysts for trichloroethene hydrodechlorination, *Environ. Sci. Technol.*, **39**, 1346-1353.
- 96 Borgna, A., Anderson, B.G., Saib, A.M., Bluhm, H., Havecker, M., Knop-Gericke, A., Kuiper, A.E.T., Tamminga, Y. and Niemantsverdriet, J.W. (2004) Pt-Co/SiO₂ Bimetallic Planar Model Catalysts for Selective Hydrogenation of Crotonaldehyde, *J. Phys. Chem. B*, **108**, 7905.
- 97 Renouprez, A., Faudon, J.F., Massardier, J., Rousset, J.L., Delichère, L. and Bergeret, G. (1997) Properties of supported PdNi catalysts prepared by coexchange and organometallic chemistry, *J. Catal.*, **170**, 181.

- 98 Zhu, L., Liang, K.S., Zhang, B., Bradley, J.S. and DePristo, A.E. (1997) Bimetallic PdCu catalysts: X-ray diffraction and theoretical modeling studies, *J. Catal.*, **167**, 412.
- 99 Shen, J., Hill, J.H., Watve, R.M., Spiewak, B.E. and Dumesic, J.A. (1999) Microcalorimetric, infrared spectroscopic, and DFT studies of ethylene adsorption on Pt/SiO₂ and Pt-Sn/SiO₂ catalysts, *J. Phys. Chem. B*, **103**, 3923.
- 100 Hill, J.M., Shen, J., Watve, R.M. and Dumesic, J.A. (2000) Microcalorimetric, infrared spectroscopic, and DFT studies of ethylene adsorption on Pd and Pd/Sn, *Catal. Langmuir*, **16**, 2213.
- 101 Deutsch, S.E., Miller, J.T., Tomoshige, K., Iwasawa, Y., Weber, W.A. and Gates, B.C. (1996) Supported Ir and Pt Clusters: Reactivity with oxygen investigated by extended X-ray absorption fine structure spectroscopy, *J. Phys. Chem. B*, **100**, 13408.
- 102 Reifsnnyder, S.N., Otten, M.M., Sayers, D.E. and Lamb, H. (1997) Hydrogen chemisorption on Silica-supported Pt clusters: In situ X-ray absorption spectroscopy, *J. Phys. Chem.*, **101**, 4972.

Final manuscript received in January 2006

Copyright © 2006 Institut français du pétrole

Permission to make digital or hard copies of part or all of this work for personal or classroom use is granted without fee provided that copies are not made or distributed for profit or commercial advantage and that copies bear this notice and the full citation on the first page. Copyrights for components of this work owned by others than IFP must be honored. Abstracting with credit is permitted. To copy otherwise, to republish, to post on servers, or to redistribute to lists, requires prior specific permission and/or a fee: Request permission from Documentation, Institut français du pétrole, fax. +33 1 47 52 70 78, or revueogst@ifp.fr.